Resource

Cell Reports

An NLRP3 Mutation Causes Arthropathy and Osteoporosis in Humanized Mice

Graphical Abstract

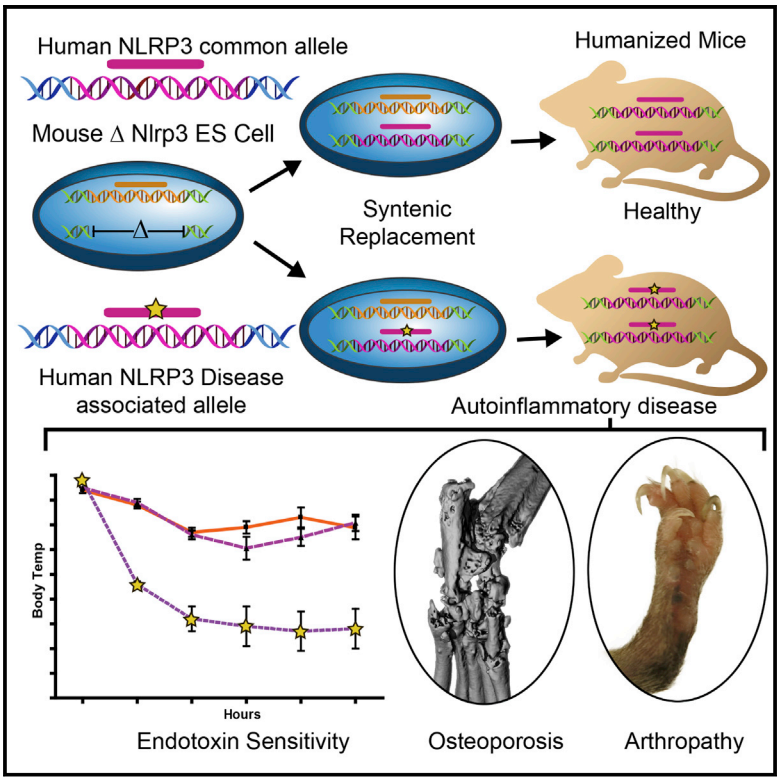

Highlights

- Syntenic replacement humanizes the NLRP3 inflammasome in mice
- The common *NLRP3* gene replaces the function of the excised mouse gene
- An NLRP3 disease allele causes arthritis, osteoporosis, and endotoxin hypersensitivity
- NLRP3-humanized mice provide a platform for evaluating anti-NLRP3 therapies

Authors

John N. Snouwaert, MyTrang Nguyen, Peter W. Repenning, ..., Ted A. Bateman, Jenny P.-Y. Ting, Beverly H. Koller

Correspondence

bkoller@correspondence.unc.edu

In Brief

In this study, Snouwaert et al. use syntenic replacement to generate the first mouse model in which human rather than mouse NLRP3 triggers inflammasome assembly. Introduction of a gain-of-function mutation into the humanized locus results in development of progressive arthritic disease in adult animals.

Snouwaert et al., 2016, Cell Reports *17*, 3077–3088
December 13, 2016
http://dx.doi.org/10.1016/j.celrep.2016.11.052

CellPress

Cell Reports
Resource

An NLRP3 Mutation Causes Arthropathy and Osteoporosis in Humanized Mice

John N. Snouwaert,[1,5] MyTrang Nguyen,[1,5] Peter W. Repenning,[1] Rebecca Dye,[1] Eric W. Livingston,[4] Martina Kovarova,[1] Sheryl S. Moy,[2] Brian E. Brigman,[3] Ted A. Bateman,[4] Jenny P.-Y. Ting,[1] and Beverly H. Koller[1,6,*]
[1]Department of Genetics, University of North Carolina at Chapel Hill, Chapel Hill, NC 27599, USA
[2]Department of Psychiatry, University of North Carolina at Chapel Hill, Chapel Hill, NC 27599, USA
[3]Department of Orthopedic Surgery and Pediatrics, Duke University, Durham, NC 27705, USA
[4]Department of Biomedical Engineering, University of North Carolina at Chapel Hill, Chapel Hill, NC 27599, USA
[5]Co-first author
[6]Lead Contact
*Correspondence: bkoller@correspondence.unc.edu
http://dx.doi.org/10.1016/j.celrep.2016.11.052

SUMMARY

The NLRP3 inflammasome plays a critical role in host defense by facilitating caspase I activation and maturation of IL-1β and IL-18, whereas dysregulation of inflammasome activity results in autoinflammatory disease. Factors regulating human NLRP3 activity that contribute to the phenotypic heterogeneity of NLRP3-related diseases have largely been inferred from the study of *Nlrp3* mutant mice. By generating a mouse line in which the NLRP3 locus is humanized by syntenic replacement, we show the functioning of the human NLRP3 proteins in vivo, demonstrating the ability of the human inflammasome to orchestrate immune reactions in response to innate stimuli. Humanized mice expressing disease-associated mutations develop normally but display acute sensitivity to endotoxin and develop progressive and debilitating arthritis characterized by granulocytic infiltrates, elevated cytokines, erosion of bones, and osteoporosis. This NLRP3-dependent arthritis model provides a platform for testing therapeutic reagents targeting the human inflammasome.

INTRODUCTION

Cryopyrin (NLRP3) is a large protein with distinct domains to which unique functions have been assigned. These include the N-terminal effector domain, the Pyrin domain for binding downstream signaling molecules, a nucleotide binding/oligomerization domain, a winged helix domain, a superhelical domain, and a C-terminal leucine-rich repeat receptor domain (Ting et al., 2008). Perturbation of cell homeostasis alters the secondary/tertiary structure of the protein, resulting in oligomerization of the cytoplasmic monomers (Martinon et al., 2002). The structural changes allow the NLRP3 pyrin domains of the complex to associate with the bipartite protein PYCARD. The CARD domain of PYCARD becomes available to interact with pro-caspase 1 and 11, leading to proximity-dependent self-cleavage of the pro-enzymes into their active forms (Agostini et al., 2004). A primary function of these caspases is proteolytic processing of pro-interleukin 1β (IL-1β) and pro-IL-18 to their biologically active forms, IL-1β and IL-18, a prerequisite for their release from intact cells (Dinarello, 2009). The majority of our knowledge concerning the function of this important innate immune pathway in human disease has been extrapolated from mouse studies in which the immune response of wild-type (WT) mice is compared with that in mice lacking these proteins (Elliott and Sutterwala, 2015). Direct studies of the response of the human protein have largely been limited to the study of transformed myeloid cell lines and primary immune cell populations. Studies using macrophages from WT and NLRP3-deficient mice have identified a diverse and extensive list of agents that lead to NLRP3-dependent release of IL-1β from cells, including not only microbial agents such as bacteria, toxins, and fungi but also particulate matter such as urate crystals, asbestos, alum, silica, amyloid β, and ATP (Leemans et al., 2011). It is largely presumed that these same agents can trigger assembly of the human inflammasome and thus initiate and/or amplify inflammatory responses in humans.

Mutations in *NLRP3* have been identified in most patients with autoinflammatory disorders, including familial cold autoinflammatory syndrome (FCAS), Muckle-Wells syndrome (MWS), chronic infantile neurological cutaneous and articular syndrome (CINCA), and neonatal onset multisystem inflammatory disease (NOMID) (Kastner et al., 2010). Identification of mutations in the same gene suggests that these syndromes represent a disease spectrum, with the severity of the disease likely related to the degree to which a particular mutation alters the structure and various functions of the protein (Aksentijevich et al., 2007). Collectively termed cryopyrin-associated periodic syndromes (CAPS), these diseases share many symptoms, including rash, episodic unprovoked fever, abdominal pain, elevated acute-phase proteins, fatigue, redness of the eyes, and arthralgia. Both the intensity and the frequency of the symptoms can vary, with the most severe disease resulting in bone deformities, hearing loss, mental impairments, and organ damage (Stojanov and Kastner, 2005). The majority of CAPS-associated mutations map to an inner surface of the hexameric ring in the cryopyrin model. It is hypothesized that the mutations disrupt the closed

form of the monomeric protein (Aksentijevich et al., 2007), leading to inappropriate assembly of the NLRP3 complex in the absence of a second signal and subsequent release of IL-1β and IL-18 (Agostini et al., 2004).

The primary structure of NLRP3 is well conserved between mouse and human, allowing animal models of CAPS to be generated by introducing the disease-associated mutations into the mouse gene (Bonar et al., 2012; Brydges et al., 2009; Meng et al., 2009). Important characteristics of the human disease are reiterated in these models, including autoinflammatory disease accompanied by elevated production of IL-1β. However, the inflammatory disease reported is more severe than that observed in patients with comparable mutations. Most of the mice inheriting *Nlrp3* genes harboring CAPS mutations die before adulthood. In addition, the severity of the inflammatory disease associated with particular mutations does not correlate well with the effects of the corresponding mutations in humans. For example, a FCAS-associated mutation, which represents the mildest CAPS in humans, results in early lethality in mice, whereas a higher percentage of the mice carrying MWS-associated mutations survive past weaning.

Differential impact of a given amino acid substitution in proteins of two different species is perhaps not surprising. Epistasic interactions can occur both within and between molecules, and the effect of individual mutations may depend on the genetic context in which they occur (Lehner, 2011; Camps et al., 2007). The position of the amino acid substitution in NLRP3 is certainly a key determinant of the impact on its function. But this impact is likely to be further defined by primary interactions between neighboring amino acids and by secondary and tertiary interactions with more distant peptide motifs. Thus, the effects of introducing a mutation corresponding to a human disease-associated polymorphism into the murine homolog of the affected protein might be expected, in some cases at least, to differ substantially from those responsible for the human disease. An interesting example of this is the impact of the loss of residue 508 on CFTR. This deletion mutation dramatically alters the stability and function of the human protein, whereas both the swine and mouse Δ508 proteins show some activity (Ostedgaard et al., 2007). Perhaps the best evidence supporting the importance of epistasis in determining the physiological consequence of non-synonymous mutations comes from the observation that, in some cases, these disease-associated residues occur as the wild-type residues in functionally orthologous proteins (Baresić et al., 2010; Kondrashov et al., 2002). Intramolecular epistatic interactions will limit the ability to directly compare the impact of different CAPS-associated mutations and common variants on the functions of the NLRP3 protein by generation of mutant mouse *Nlrp3* alleles.

To develop a platform for the study of common as well as CAPS-associated variants of human NLRP in vivo, we have generated a mouse line in which the mouse *Nlrp3* locus is excised and replaced with either a common allele or a disease-associated human *NLRP3* allele. We report here the functioning of the human *NLRP3* human gene in the place of the mouse gene and the development of disease in juvenile and adult mice carrying a CAPS-associated, non-synonymous SNP.

RESULTS

Generation of Mice Carrying the Human NLRP3 Locus

An embryonic stem cell (ESC) line in which the 35-kb mouse *Nlrp3* locus is deleted and the establishment of co-isogenic 129S6 mice carrying this deletion have been described previously (Kovarova et al., 2012). We refer to this mutation as *ΔNlrp3* to distinguish this line from other NLRP3-deficient mouse lines that still contain *Nlrp3* introns and exons. *ΔNlrp3* ES cells were used to generate an ESC line in which the deleted DNA was replaced with a single copy of the corresponding syntenic *NLRP3* DNA (Figure 1A). This 48,199-base pair (bp) DNA segment includes ~12 kb of DNA 5′ to the ATG site, all *NLRP3* introns and exons, and 3′ intragenic DNA. The human gene is present as a single copy, the orientation and relative distance of *NLRP3* to the endogenous murine upstream and downstream genes is preserved, and, with the exception of a mutant loxP and frt site, no vector or marker sequences remain in the humanized locus. These ESCs were used to generate co-isogenic 129S6-*NLRP3* mice. Using standard nomenclature, the human gene is capitalized (*NLRP3*), whereas *Nlrp3* refers to the mouse gene.

Evaluation of the Expression of *NLRP3* in the Mouse

Tissues and cells were collected from mice heterozygous for a WT mouse and human gene, referred to as *NLRP3*/*Nlrp3* mice, as well as from animals homozygous for either the mouse or human gene. Human *NLRP3* was robustly expressed in a pattern that generally followed that of the mouse gene (Figure 1B). The only exception was in neutrophils, in which *NLRP3* expression was significantly lower than that of *Nlrp3*, suggesting that regulation of the human and mouse genes may differ in these cells. To further examine *NLRP3*/*Nlrp3* expression, we measured changes in mRNA levels in peritoneal macrophages after lipopolysaccharide (LPS) exposure. Both mouse and human NLRP3 mRNA levels showed a rapid but transient increase after stimulation (Figure 1C). In contrast, evaluation of parallel LPS-stimulated cultures with an NLRP3-specific antibody reported to interact with both human and mouse protein suggests that not only are the levels of NLRP3 in the humanized mice lower in resting cells, but the levels achieved on stimulation of the cells with LPS are lower and may decrease more rapidly after stimulation, suggestive of differences in the stability and or regulation of the human and mouse proteins (Figure 1D).

Functioning of the Human NLRP3 Inflammasome in Mouse Macrophages

To determine whether the human gene could restore NLRP3 function in mice, we examined whether mice in which the Δ locus had been restored with the human gene could produce IL-1β in response to stimuli that have been shown previously to be NLRP3-dependent. Peritoneal macrophages from WT, *ΔNlrp3*/*ΔNlrp3*, and 129 *NLRP3*/*NLRP3* mice were exposed to LPS to induce IL-1β production and then to alum, silica, uric acid crystals, imidazoquinoline compounds, or ATP. In addition, cells were exposed to nigericin, a pore-forming agent that stimulates the NLRP3 inflammasome by depleting intracellular K^+ (Solle et al., 2001). The human gene restored the response of the

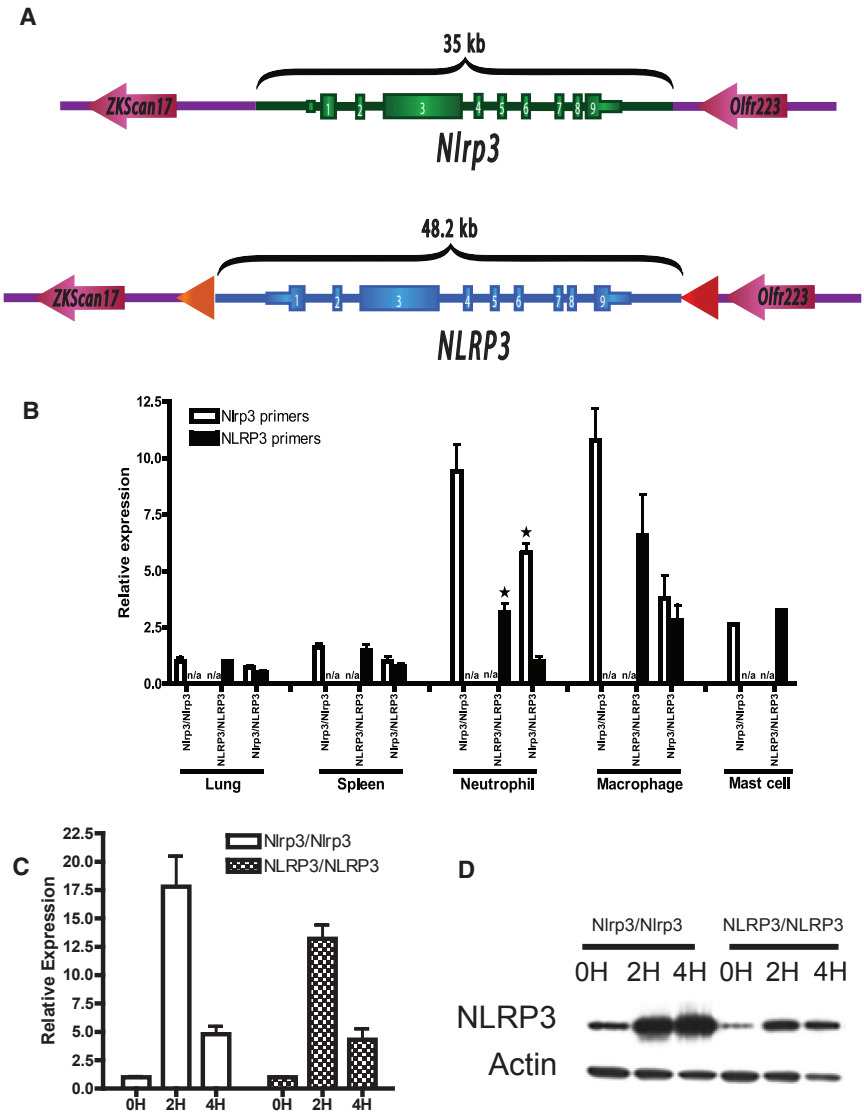

Figure 1. Syntenic Replacement of *Nlrp3* and Expression of *NLRP3* in Mice Heterozygous and Homozygous for the Replaced Locus

(A) Schematic comparing the WT mouse *Nlrp3* locus on chromosome 11 and the locus present in the *NLRP3* animals. Note that the relative position of the 5′ and 3′ neighboring genes has been maintained. The upstream transition from mouse to human DNA is marked by a mutant loxP site (gold arrow), whereas that at the downstream site of transition is marked with an frt site (red arrow). The larger segment of DNA inserted versus DNA deleted reflects differences in intron length between the human and mouse genes. The upstream region of human DNA includes elements identified that are likely to be involved in the regulation of gene expression, such as the 3,600-bp 5′ of the ATG analyzed by Anderson et al. (2008).

(B) Expression of *NLRP3* and *Nlrp3* in the indicated tissues was assessed by qPCR normalizing to 18S RNA. Each of the primer sets was species-specific, and expression is shown as fold change relative to levels in the lung. Expression of the human gene is generally lower, but this only achieves statistical significance in neutrophils. Results are expressed as mean ± SEM, $p < 2 \times 10^{-5}$, n = 3 for each genotype.

(C and D) Peritoneal macrophages of the indicated genotype were cultured for 0, 2, or 4 hr in the presence of 1 μg/mL LPS.

(C) NLRP mRNA levels were determined by qPCR, and changes in *NLRP3*/*Nlrp3* expression were compared with levels observed at the 0-hr time point, which was assigned a value of 1.

(D) Lysates prepared from parallel cultures were evaluated by western blot using an antibody capable of recognizing both human and mouse NLRP3.

mouse macrophages to these various agents (Figure 2). As reported previously, a robust release of IL-1β was observed in response to silica (Cassel et al., 2008); monosodium urate (MSU), an etiological agent in gout; or calcium pyrophosphate dihydrate (CPPD) crystals (Martinon et al., 2006). The humanized cells released IL-1β in response to all agents that triggered IL-1β production by mouse NLRP3, although the response was significantly lower, except in the case of MSU treatment. The response to MSU did not differ between humanized and WT macrophages. As expected, an NLRP3-dependent release of IL-1β was observed in response to ATP in the humanized cells, although, while the response was robust, it was significantly lower than that observed with mouse macrophages. We did not detect release of IL-1β in response to the imidazoquinoline compounds R837 and R848. This is not surprising because the level of IL-1β released on exposure to these agents is very low (Kanneganti et al., 2006).

Generation of an ESC Line Carrying the *NLRP3*^{D305N} Allele

A second ESC line was generated that differed from that described above only in that the autoinflammatory disease-associated D305N SNP was introduced into the DNA used to restore the *ΔNlrp3* locus (numbering is based on uniprot.org, and this SNP is often referred to as D303N) (Figure S1A). We expect the missense mutation to be the only difference between this mouse line and that described above. Heterozygous pups were present in litters at the expected frequency and displayed no apparent phenotype. No difference was seen in the expression of the two genes in various tissues or in LPS-treated macrophages (Figures S1B and S1C). This is not surprising given that the strategy used to generate the two lines ensures that the only difference between the two mouse ES cell lines is the SNP encoding D305N. For simplicity, we refer to the 129S6-*NLRP3*^{D305N} mouse as D305N.

The pro-inflammatory characteristics of this disease-associated *NLRP3* variant were examined by exposure of macrophages to LPS (Figure 3). As expected, only low levels of IL-1β were detected in supernatants from macrophages carrying the

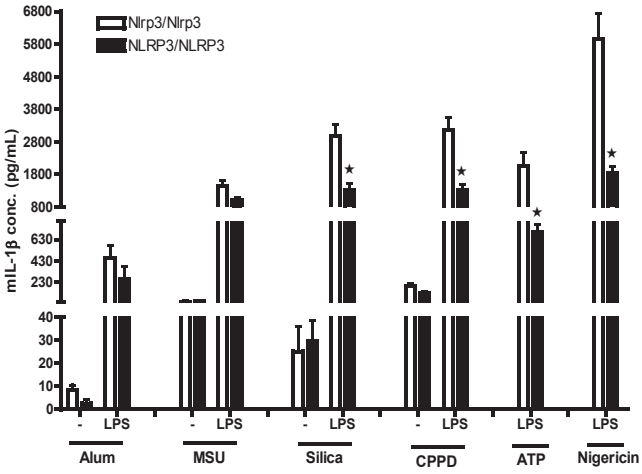

Figure 2. Comparison of the Activity of Human and Mouse NLRP3-Containing Inflammasomes

Peritoneal macrophages from mice of the indicated genotypes were exposed to LPS for 6 hr to induce expression of IL-1β and then to the indicated agent for an additional 6 hr with the exception of ATP. Cells were exposed to 5 mM ATP for 30 min immediately prior to the end of the experiment. IL-1β release was measured by ELISA. No signal was detected in supernatants from *ΔNlrp3* cells. Although cells from the humanized mice responded to all agents tested, the response was slightly less robust than that of the *Nlrp3/Nlrp3* cells, and this decrease was significant in some cases. Results are expressed as mean ± SEM, n = 3, *p < 0.05.

common human *NLRP3* gene. In contrast, robust release of IL-1β was observed in the supernatant from macrophages carrying the D305N mutation at all LPS concentrations (Figure 3A). Addition of ATP resulted in the expected increase in IL-1β release from LPS-primed macrophages expressing the common *NLRP3* allele, and, after exposure to this agent, the levels of IL-1β in the supernatant of the control and mutant cultures were not significantly different (Figure 3B). To determine whether activation of the D305N inflammasome by a priming signal alone was unique to LPS, this experiment was repeated using tumor necrosis factor α (TNF-α) as the priming signal (Figure 3C). Similar to LPS, TNF-α alone was sufficient to induce IL-1β release by macrophages carrying the CAPS mutation. However, the magnitude of the release was smaller than that observed on exposure to LPS, and the release of IL-1β from the mutant cells could be further enhanced by exposure to a second stimulus, in this case ATP.

Response of D305N and NLRP3 Mice to LPS

The in vivo response of mice expressing common and mutant *NLRP3* to LPS was examined first in congenic 129B6F1 animals of three different genotypes. Each mouse carried the *ΔNlrp3* locus on the C57BL/6-derived chromosome and one of three different alleles on the 129-derived chromosome: WT (*Nlrp3/ΔNrlp3*), the common *NLRP3* allele (*NLRP3/ΔNlrp3*), or the disease associated variant (D305N/*ΔNlrp3*). Mice of each of the three genotypes were present in litters at expected frequencies and could not be distinguished by observation alone. Mice were exposed intraperitoneally (i.p.) to a low dose (2.5 mg/kg)

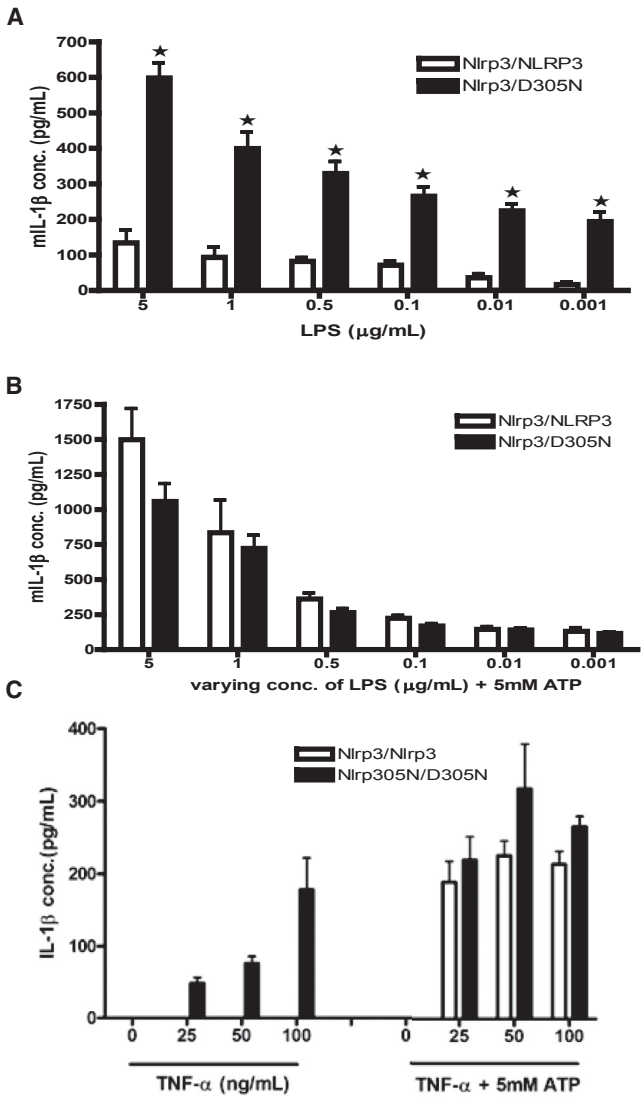

Figure 3. D305N-Expressing Peritoneal Macrophages Release IL-1β in Response to LPS without a Second Stimulus

Thioglycollate-elicited peritoneal macrophages were collected from *Nlrp3/NLRP3* and *D305N* F1 mice.

(A) Cells were incubated with increasing concentrations of LPS, supernatant was collected 24 hr later, and IL-1β levels were determined. p < 0.001 for all LPS concentrations.

(B) No difference was observed in the ability of the two populations to release IL-1β in response to ATP after priming with LPS.

(C) Cells were incubated with increasing concentrations of TNF-α. Supernatant was collected 24 hr later, and IL-1β levels were determined. In a parallel experiment, ATP (5 mM) was added 30 min before the collection of medium. IL-1β in supernatants from normal peritoneal cells was below the level of detection. p > 0.001 for all TNF-α concentrations. No difference was observed in the ability of the two populations to release IL-1β in response to TNF-α and ATP.

Results are expressed as SEM, n = 5.

of LPS, and the ensuing hypothermic shock was monitored over 8 hr. A small but significant drop in temperature was measured in the *Nlrp3/ΔNlrp3* and *NLRP3/ΔNlrp3* mice

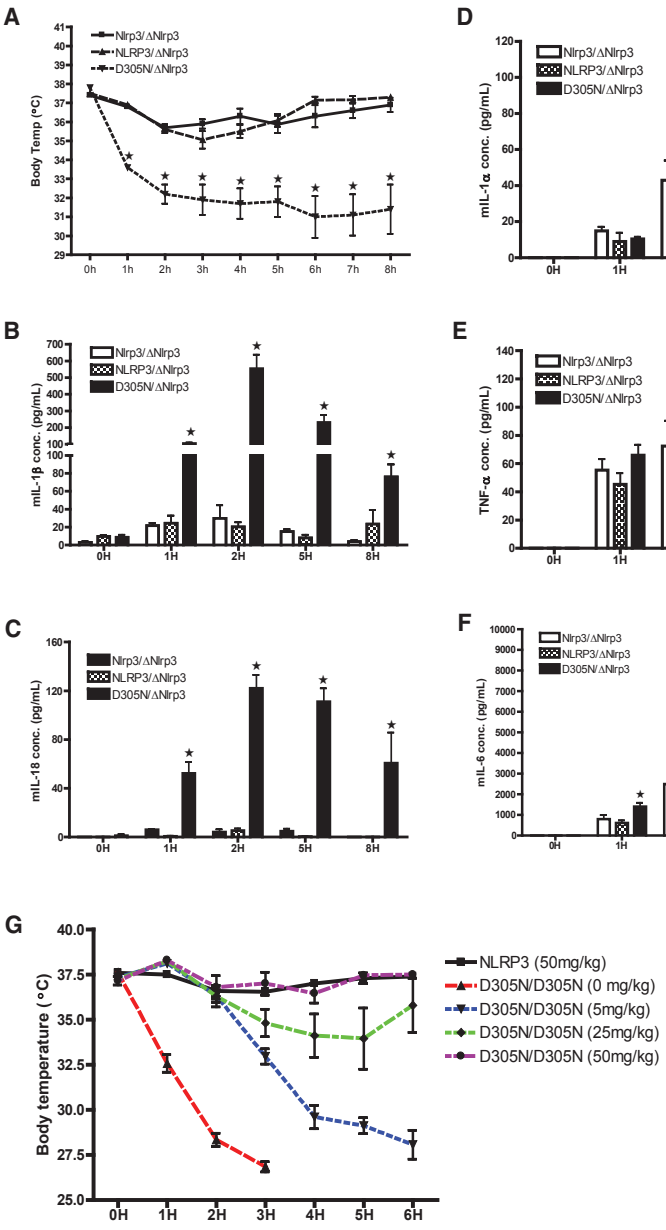

Figure 4. Response of Mice Expressing *Nlrp3*, *NLRP3*, or *D305N* to LPS

(A) Mice of the indicated genotype received a low dose (2.5 mg/kg) of LPS i.p., and the core body temperature was monitored for 8 hr.

(B–F) Cytokine levels in the peritoneal fluid were determined in an identically treated cohort at the indicated time points. Mice carrying a single copy of the D305N mutation showed a dramatic hypothermic response accompanied by an early increase in (B) IL-1β and (C) IL-18 production and later increases in (D) IL-1α, (E) TNFα, and (F) IL-6.

(G) The rapid drop in temperature observed in the D305N mice was attenuated by pretreatment with the small-molecule NLRP inhibitor CRID3/MCC. Results are expressed as mean ± SEM, n = 4.

(Figure 4A). The magnitude and the time course were similar in mice carrying a single copy of the human or mouse gene. In contrast, a dramatic hypothermic response was apparent 1 hr after LPS exposure of mice expressing the *NLRP3* D305N variant, and these animals remained hypothermic through the duration of the experiment. In a parallel experiment, peritoneal exudate was collected and evaluated for the production of cytokines (Figures 4D–4F). In animals expressing the WT mouse and the common *NLRP3* allele, a small but significant increase in the level of this cytokine was observed. In contrast, a dramatic increase in the levels of IL1β and IL-18 (Figures 4B and 4C) was observed in exudates collected from D305N animals 1 hr after LPS exposure. Levels continued to increase, peaking 2 hr after treatment, and achieved concentrations 20-fold higher than those observed in mice expressing either normal human or mouse *NLRP3.* Other inflammatory mediators associated with LPS-mediated sepsis, but which are not dependent on the inflammasome for processing and release, including IL-1α (Figure 4D), TNF-α (Figure 4E), and IL-6 (Figure 4F), were present at significantly higher levels in the exudate collected from D305N animals. The dramatic hypotheric response to LPS of the D305N mice provides a sensitive and rapid means of evaluation of the in vivo efficacy of small-molecule inhibitors of NLRP3. To demonstrate this, we evaluated the recently described NLRP3 inhibitor CRID3. A dose-dependent attenuation of hypothermia was observed in D305N mice treated with the compound prior to LPS exposure, with complete protection observed at 50 mg/kg (Figure 4G).

Characterization of Mice Homozygous for the D305N Mutation

Mice homozygous for the D305N mutation were present in litters at the expected frequency and did not differ in size from WT littermates. Analysis of a cohort of 6-month-old co-housed 129S6 and D305N/D305N mice showed a slight decrease in weight that did not achieve statistical significance, and the D305 mice occasionally developed blepharitis. No hepatomegaly was apparent; however, significant splenomegaly was observed in the mutant animals (Figure S2). Analysis of splenocytes with CD4, CD8, CD11b, CD69, and Gr-1 indicated that neither the lymphocyte numbers nor the CD4+/CD8+ ratio were altered in the mutant mice. Expression of CD69, an early marker of activation was also not increased in this population. However, the fraction of CD11b+ Gr1+ myeloid cells, which is composed of activated monocytes and granulocytes, was dramatically higher in the D305N mice.

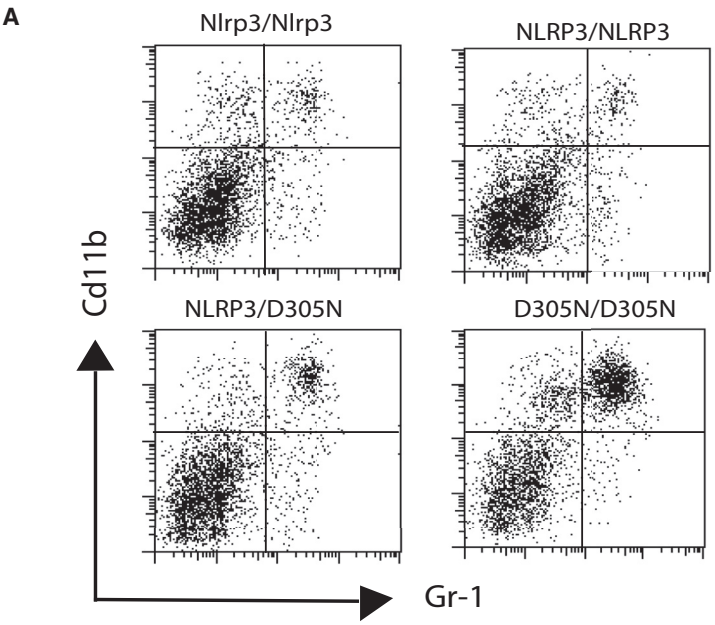

	% Surface markers				
Mice	CD4	CD8	CD4_CD8	B220	CD11b_GR-1
Nlrp3/Nlrp3	19.5 ± 1.9	12.2 ± 1.5	0.9 ± 0.1	38.5 ± 1.1	1.1 ± 0.09
NLRP3/NLRP3	19.9 ± 1.6	12.8 ± 0.5	1.3 ± 0.3	37.4 ± 2.7	1.0 ± 0.2
NLRP3/D305N	19.5 ± 1.3	11.9 ± 1.0	1 ± 0.1	34.1 ± 1.7	10.6 ± 1.9*
D305N/D305N	10.3 ± 1.8*	6.1 ± 0.9*	1 ± 0.1	25.9 ± 2.6*	28.7 ± 3.5*

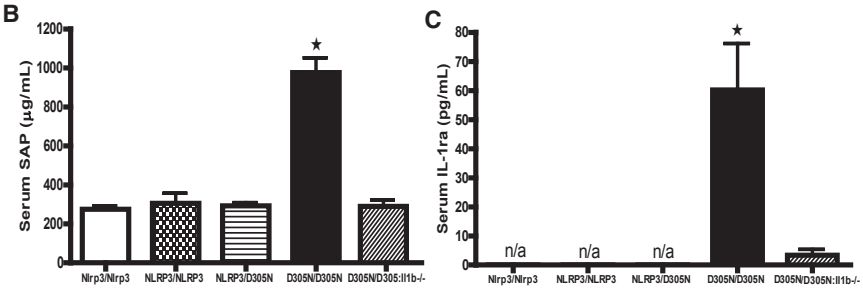

Figure 5. Increase in Myeloid Cells in Spleens from D305N/D305N Mice

(A) An approximately 25-fold increase in the percentage of CD11b/GR-1-positive cells was observed in spleens from D305N/D305N mice. A small but significant increase in this population was also observed in D305N/NLRP3 ($n = 3$, $p < 0.05$).

(B) Increase in major acute-phase protein. SAP component levels were determined by ELISA in 5-month-old co-housed mice of the indicated genotype ($n = 3$, $^*p = 0.01$).

(C) Serum IL-1ra in 2-month-old co-housed male mice of the indicated genotype ($n = 4$, $^*p = 0.03$).

This population represented approximately 1% of splenocytes from WT animals, whereas approximately 10% of cells in the D305N mice were CD11b+ Gr-1+ (Figure 5A). Consistent with the presence of an ongoing inflammatory response in the D305N/D305N mice, levels of the major acute-phase protein, serum amyloid P, were elevated in the D305N animals (Figure 5B), as were serum levels of the natural IL-1β antagonist, IL1RA (Figure 5C). Hematological parameters were assessed in co-housed mice with the following genotypes: *Nlrp3/Nlrp3*, *NLRP3/NLRP3*, *ΔNlrp3/ΔNlrp3*, *Nlrp3*/D305N, and D305N/D305N (Table S1). White cell counts (WBC) were higher in mice heterozygous and homozygous for the mutant allele, although the increase was modest in the *Nlrp3*/D305N mice and did not achieve significance with this group size ($n = 3$). The WBC of the D305N mice was more than 6-fold higher than that of control groups. This reflected a modest but significant increase in lymphocytes and monocytes and a large but variable increase in circulating granulocytes. Histological evaluation of the sagittal section of the brain showed inflammation of the meninges in the D305N mice (Figure S3), although no deficit in hearing could be documented (Figure S4). Staining of organs with Congo red revealed no deposits of amyloid in the kidney or brain. To determine whether the inflammatory changes observed in the D305N mice were mediated by IL1β, we generated D305N/D305N:Il1b$^{-/-}$ mice. Not only was the spleen size normal in these animals (Figure 2S), but serum amyloid P (SAP) and IL1RA levels were no longer elevated (Figures 5B and 5C).

Development of Arthropathy

Although not observed at weaning, arthritic changes in the limbs and paws of the D305N/D305N mice became apparent within the first 3 months of life and progressed as the mice aged (Figure 6A). To examine this further, myeloperoxidase (MPO) activity, which is high in mature neutrophils and relatively specific for this cell type, was assessed non-invasively using a chemiluminescent reagent. No signal was observed at the joints and paws of control animals, whereas luminescence was easily detected at the joints of the mutant mice (Figure 6B). To examine further the inflammation present at the joints, a cohort of mice was euthanized, and cytokines present in tissue homogenates prepared from the paws were analyzed. IL-1β, which could not be detected in the lysates prepared from paws of normal mice, was elevated in the samples from the mutant animals. IL-18 and IL-6 levels were significantly higher, as were the levels of the IL-1β receptor antagonist IL-1RA (Figure 6C). Levels of IL-17 and IL-23 in homogenates from both mutant and WT animals were below the sensitivity of the assay. To determine whether the swelling of the paws corresponded with edema formation, serum protein

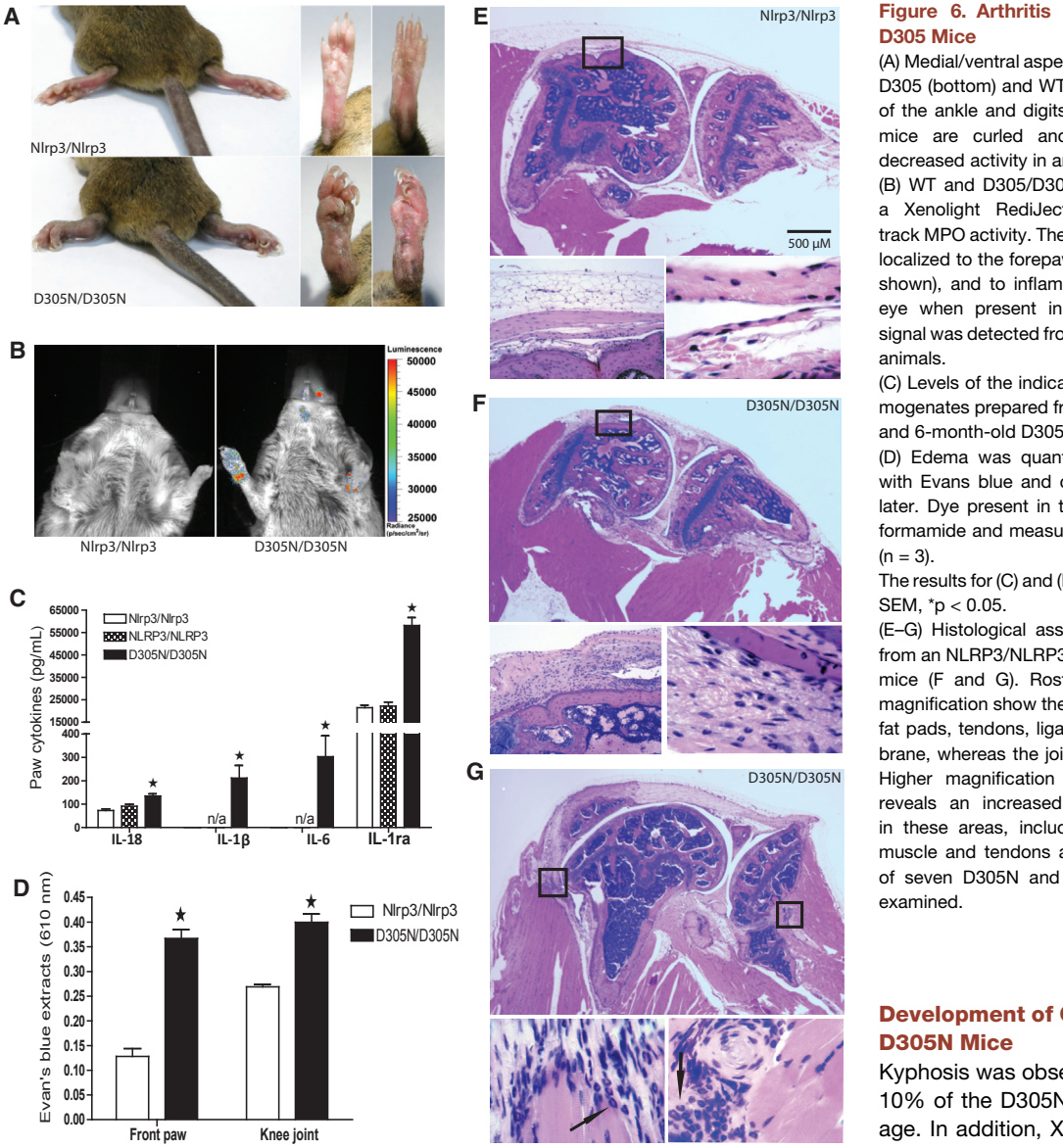

Figure 6. Arthritis Development in D305/D305 Mice

(A) Medial/ventral aspect of the hindpaws of D305/D305 (bottom) and WT (top) mice shows swelling of the ankle and digits. The claws of the mutant mice are curled and longer, likely reflecting decreased activity in arthritic animals.

(B) WT and D305/D305 mice were injected with a Xenolight RediJect inflammation probe to track MPO activity. The chemiluminescence signal localized to the forepaws and hindpaws (data not shown), and to inflammatory lesions around the eye when present in D305N/D305N mice. No signal was detected from the extremities of control animals.

(C) Levels of the indicated cytokines in tissue homogenates prepared from the autopods of control and 6-month-old D305N/D305N mice (n = 4).

(D) Edema was quantified by injection of mice with Evans blue and collection of tissue 30 min later. Dye present in tissue was extracted using formamide and measured spectrophotometrically (n = 3).

The results for (C) and (D) are expressed as mean ± SEM, *p < 0.05.

(E–G) Histological assessment of the knee joint from an NLRP3/NLRP3 mouse (E) and two D305N mice (F and G). Rostro-lateral sections at low magnification show the increased cellularity of the fat pads, tendons, ligaments, and synovial membrane, whereas the joint space is largely spared. Higher magnification of the indicated regions reveals an increased number of granulocytes in these areas, including the junction between muscle and tendons and tibial turbosity. A total of seven D305N and seven control mice were examined.

extravasation into the paws and knee joints was quantified using Evans blue. Significant increases in serum protein levels were observed in both the front paws and knee joints (Figure 6D). Histological evaluation of the knee showed the presence of cellular infiltrate in soft tissues, including entheses—sites where tendons, ligaments, joint capsules, and muscles connect to bone. These infiltrates contained large numbers of granulocytes, identified based on their segmented nuclei (Figures 6E–6G). Although hyperplasia of the synovium was observed, inflammatory cells were not present in the joint space, and no loss of articulating cartilage was apparent on this analysis. Infiltrating granulocytes and mononuclear cells were also abundant in the entheses, ligaments, and fibrous capsule of tendons of the paw, particularly in the soft tissue of the digits, where bone loss was also observed (Figure S5). In contrast, no visible changes in the joints of the D305N/D305N:Il1b$^{-/-}$ animals were observed.

Development of Osteoporosis in D305N Mice

Kyphosis was observed in approximately 10% of the D305N mice with advancing age. In addition, X-rays of the hindlimbs showed increased radiolucency and thinner cortices in all visualized bones of mice carrying the D305N allele relative to those of control mice (Figure 7A). This is consistent with osteoporosis, which may be either a primary condition or secondary to inflammation, decreased use, or both. Microcomputed tomography (microCT) followed by three-dimensional reconstruction was used to further characterize changes in the bone microarchitecture of the NLRP3 mutant animals (Figure 7B). Although D305N mice showed no differences relative to mice humanized with the common NLRP3 allele in the amount or density of trabecular bone at the proximal tibia, they showed a significant decrease in connectivity density and a significant increase in trabecular thickness (Table S2; Figures S1–S6), suggesting a compensatory response to the loss of trabecular connections. Compared with control mice, D305N mice had less cortical bone, and it was more porous. The medullary/marrow cavity and "footprint" of cortical bone in these animals was also smaller, contributing to a 33%

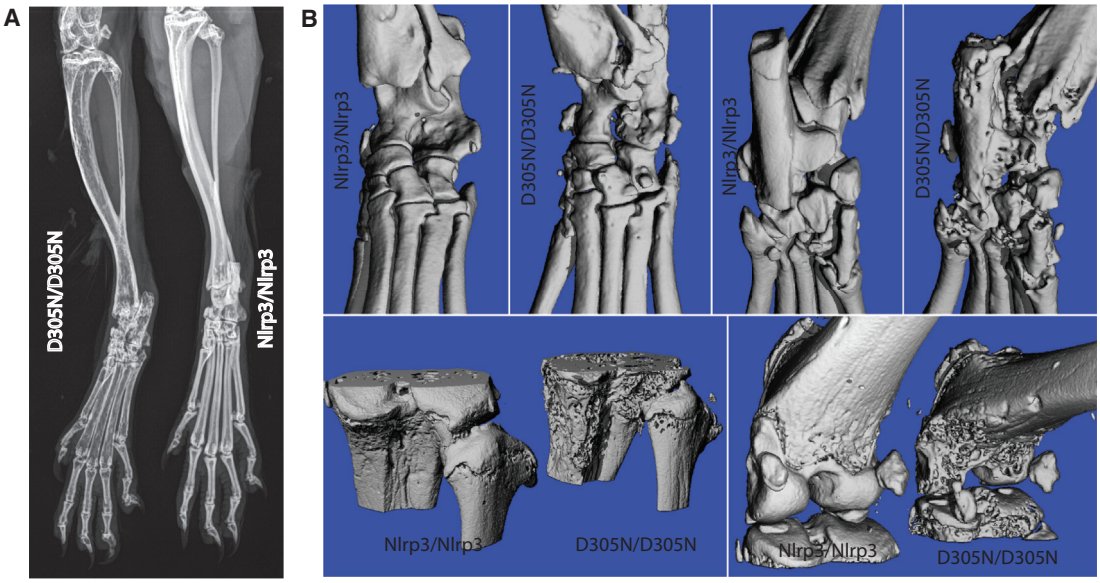

Figure 7. Radiographic Evaluation of Hindlimbs from Wild-Type and D305N/D305N Mice
(A) X-ray of the hindlimbs of mutant and WT animals 9 months of age showing bone loss in aging D305N mice.
(B) MicroCT of the ankle bones of WT and D305N/D305N animals.

lower polar moment of inertia, meaning that the femur has a lower ability to resist torsional and bending loads. A small but significant decline of tissue mineral density was observed, suggesting that material properties may also be negatively affected in D305N mice. Lower mineral density is also indicative of greater bone turnover, consistent with a greater activation of osteoclasts and a general state of systemic inflammation (Table S2).

Articular subchondral erosion was prominent in both the ankles and knees of the D305N mice (Figure 7B). To rule out possible developmental differences in bone density, X-ray and microCT analysis of D305N mice were carried out at 6 weeks of age. The D305N mice could not be distinguished at this age (Figures S6A and S6B) from the WT.

DISCUSSION

We have generated mice in which the mouse *Nlrp3* locus has been excised and replaced with its human counterpart. The extent to which we chose to extend the replacement of mouse sequences with corresponding human sequences upstream and downstream of the introduced human *NLRP3* gene was based on striking a balance between two goals. The first was to maximize the likelihood that the expression pattern of the introduced gene would mimic that of the human gene rather than the host species, whereas the second was to avoid interfering with the normal expression of neighboring endogenous genes. The length of the flanking human sequences was therefore chosen based on available knowledge of transcriptional regulatory elements associated with *NLRP3* as well as the mouse genes flanking the replaced locus. For both human and mouse NLRP3, expression is highest in cells of myeloid lineage, with only low levels of expression detected in lymphoid cells and most organs (Anderson et al., 2004; Manji et al., 2002). This expression pattern was largely preserved in our humanized mice, indicating that the regulatory elements in the human *NLRP3* gene are recognized by the mouse *trans*-acting transcription factors that confer this pattern of expression. Of the tissues examined, only neutrophils displayed a significant difference in expression between the human and the mouse genes, with the human *NLRP3* gene being expressed at a lower level.

The humanized *NLRP3* locus provides the opportunity to directly compare the function of human and mouse NLRP3 both in primary immune cells and in vivo. Comparison of macrophages expressing the human protein with macrophages from WT littermates showed that, although LPS exposure alone was insufficient to trigger inflammasome assembly in macrophages expressing either the mouse or human protein, both the mouse and the humanized inflammasome released IL-1β in response to a similar spectrum of danger-associated molecular patterns (DAMPs). Overall, the relative ability of specific DAMPs to mediate assembly of the mouse or human NLRP3 inflammasome was well conserved. This is consistent with the hypothesis that the NLRP3 inflammasome responds to perturbations in intracellular K^+ and, thus, that the magnitude of the response reflects the ability of the particulate matter or toxin to alter cell permeability to this ion. Contrary to this model, some studies have noted differences in the contribution of NLRP3 to IL1β production by both human and mouse macrophages in response to specific stimuli (Atianand et al., 2011). However, these studies are hard to interpret because identification of equivalent cell populations for this type of study is difficult. Differences observed may not reflect differences in the cell's ability to form an inflammasome but, rather, upstream differences in the response of the cell to the pathogen-associated molecular pattern (PAMP); for example, the binding of the toxin to the

cell. The mice described here should provide a model for direct comparison of the assembly of the human and mouse NLRP3 inflammasome under different in vitro and in vivo experimental conditions in different cell populations. Although the macrophages expressing human NLRP3 responded to all DAMPs that elicited a response by WT macrophages, the magnitude of the response was generally smaller. This could be the result of lower expression of the human protein compared with the mouse protein. It is also possible that the decreased release of IL-1β reflects inefficiencies in the assembly of the human protein with other components of the inflammasome, such as caspase I. Alternatively, the reduced release may reflect an inherent difference between species revealed by direct comparison of responses mediated by WT and humanized inflammasomes. For example, it could reflect differential sensitivity of the mouse and human proteins to the changes in intracellular K^+ that trigger inflammasome assembly.

To test the suitability of our humanized NLRP3 mice as a model for examining the effects on NLRP3 function of CAPS-associated mutations or SNPs associated with common diseases such as arthritis, we generated a second mouse line from ESCs in which the *ΔNlrpr3* locus was reconstituted with an *NLRP3*-D305N locus. These mice developed a disease that modeled aspects of CAPS in humans, although the disease we observed in our D305N mice was milder than that reported for patients with the analogous mutation, which has been identified in both MWS and NOMID patients (Aksentijevich et al., 2002; Feldmann et al., 2002). This might reflect an important and interesting species difference and raises the possibility that the severe disease previously observed in mice carrying *Nlrp3* genes harboring CAPS mutations reflects subtle differences in the expression pattern of the gene in the two species and that the milder disease observed in the line described here could result from the lower expression in neutrophils. Alternatively, the observed protein levels in the humanized mice may result from species differences in NLRP3 stability. This raises the possibility that the severe disease observed upon introduction of mutations into the mouse protein results from increased duration of inflammasome activity.

Similar to all CAPS mutations, the D305N-associated autoinflammatory disease we observed in our mice was inherited in an autosomal dominant manner. Consistent with this, the response of mice carrying a single copy of the humanized locus to LPS was significantly greater than that of the WT animals. However, this heightened LPS sensitivity of the heterozygous animals did not translate into a dramatic change in their overall health under normal housing conditions. In this setting, the mice presented mild inflammation of their joints that was discernable only by evaluation of cytokines in lysates from these tissues, and, although peripheral WBC was higher, the increase was slight and did not achieve statistical significance. The phenotype of animals homozygous for the D305N locus was more severe. Similar to MWS and FCAS patients, the mice developed normally but displayed a number of features, including elevated WBC, splenomegaly, elevated serum IL-1β, and elevated acute-phase proteins characteristic of the human disease. The D305N/D305N mice responded to elevated IL-1β by increasing circulating and tissue levels of the natural receptor antagonist IL-1RA, an adaptive response also observed in CAPS (Aksentijevich et al., 2002). Interestingly, unlike CAPS patients, the D305N mice generally failed to develop skin inflammation, with skin lesions limited to a small area surrounding the eye in a very small percentage of animals later in life. The lack of inflammation in the skin might reflect differences in the regulation of the immune composition of human and mouse skin (Pasparakis et al., 2014). It is also possible that the danger signals that lead to the activation of the inflammasome in human skin are not present in our specific pathogen-free animals.

Macrophages from the D305N mice, similar to monocytes from CAPS patients, released IL-1β without the need for a second signal. We also found that this sensitizing signal was not unique to the LPS/TLR4 pathway. Exposure of D305N macrophages to TNF-α was sufficient to cause IL-1β release, consistent with a model in which assembly of the mutant inflammasome does not require a second signal rather than one in which the LPS can provide a second signal to D305N. It also indicates that inflammatory events that induce production of TNF-α may be able to trigger activation of the inflammasome in CAPS patients carrying this mutation. Elevated levels of serum TNF-α have been measured in CAPS patients, and our experiments indicate that they may contribute to an autostimulatory amplification of IL-1β production. However, the fact that this is only one of the many pathways that can provide the primary signal is shown by the limited benefit observed when treating patients with TNF-α inhibitors such as etanercept (Church et al., 2008).

We also observed arthropathy in our D305N mice that displayed both similarities and differences to that seen in CAPS patients. The acute inflammatory changes we observed, including redness, swelling, and accumulation of granulocytes, model the joint involvement observed in MWS, and the progressive bone loss we observed is consistent with the osteoporosis seen in the majority of NOMID patients. In addition, similarly to both the DIRA and NOMID patients, the articulating surface and synovial space in our D305N mice were largely spared despite extensive inflammatory infiltrate. The importance of IL-1β in osteoclast activation and inhibition of osteoblastogenesis is well documented (Redlich and Smolen, 2012). Therefore, it is not surprising that painful and swollen joints are a common symptom of MWS, whereas osteopenia and osteoporosis are observed in the majority of NOMID patients. However, although lytic bone lesions do not develop in patients with NOMID despite the increase in IL-1β production, erosion of bone at sites of inflammation is evident in both the microCT scans and histological evaluation of the D305N mice. On the other hand, deficiency of the interleukin-1 receptor antagonist (DIRA) patients present with periostitis and lytic bone lesions, and BALB/c mice lacking the orthologous mouse gene develop progressive spontaneous polyarthropathy with bone erosion (Aksentijevich et al., 2009; Horai et al., 2000; Reddy et al., 2009). Interestingly, in the IL-1RA-deficient mice, similar to the D305N mice, the synovial space was relatively free of granulocytes, and the articulation cartilage was intact (Horai et al., 2000). The lack of disease in mice on other genetic backgrounds carrying the same mutation indicates that, at least in mice, genetic modifiers can alter the pathophysiology of unregulated IL-1β activity (Nicklin et al., 2000). Similar factors may also be partially responsible for

phenotypic differences observed between humans and mice carrying various CAPS-associated mutations.

Our D305N mice also differ in several respects from previously published descriptions of mice in which CAPS-associated mutations were introduced into conserved residues in the mouse protein (Brydges et al., 2009; Meng et al., 2009). For instance, the relative severity of the disease phenotype associated with hemizygous inheritance of knockin mutations corresponding to the CAPS-associated A352V and L353P mutations was the opposite of what would have been predicted based on human studies. Although the human L353P mutation is considered milder, mice hemizygous for this mutation were either stillborn or died soon after birth (Brydges et al., 2009). In contrast, mice carrying the A352V mutation, associated with the more severe forms of disease, often survived to adulthood (Brydges et al., 2009; Meng et al., 2009). The milder form of disease observed in our D305N mice is unlikely to be specific for this mutation because introduction of the analogous mutation into the orthologous mouse codon has recently been reported to lead to death in most hemizygous animals by 2–3 weeks of age (Bonar et al., 2012). A possible explanation for the severe disease in the knockin models is that disease-associated substitutions have a greater effect on the stability and structure of the mouse protein. Subtle differences in the regulation of the expression of the human and mouse genes, such as higher expression in neutrophils, could further alter disease presentation.

In conclusion, we have used syntenic replacement to generate a mouse line that allows study of the human *NLRP3* gene in diverse primary cells and in vivo after challenge with damage-associated molecular pattern molecules. The mechanism used in generation of the mice allows introduction of mutations into both conserved and non-conserved residues of the human gene as well as into non-coding regions of the gene. Mice carrying various *NLRP3* alleles will allow direct genotype/phenotype evaluation of NLRP SNPs, including evaluation of the relative sensitivity of mutant NLRP3 proteins to environmental factors. The ease with which these mice can be bred should make it possible to generate sufficient numbers of animals to detect relatively subtle effects on inflammasome function. The mice carrying the normal and mutant proteins also provide a platform for testing drugs designed to inhibit the activity of NLRP3 because species differences in the efficacy of inhibitors are avoided.

EXPERIMENTAL PROCEDURES

Generation of the Mouse Lines

Generation of mouse ESCs and mouse lines lacking the entire 35-kb mouse *Nlrp3* locus, extending from base pair 59,534,790 to base pair 59,569,921 on chromosome 11, has been reported previously (Kovarova et al., 2012). The *ΔNlrp3* locus contains a neomycin resistance gene and the 3′ half of a human HPRT minigene preceded by a mutant loxP site. We corrected the *ΔNlrp3* locus using the 48.2-kb syntenic segment of human DNA (base pair 247,570,114 to 247,618,312 human chromosome 1 derived from BAC RP11-243D8). This DNA segment carries the common *NLRP3* allele in which codon 305 (numbering based on uniprot.org) corresponds to aspartic acid. The DNA was incorporate into a vector, referred to as a Replacer, that carries the 5′ half of the HPRT minigene followed by a mutant loxP site complementary to that in the deleted locus. Cre-mediated recombination of the Replacer vector with the deleted locus resulted in reconstitution of a selectable HPRT minigene. The same segment of DNA used in the Replacer vector was mutagenized by introducing a transition mutation at the first position of codon 305 to create the D305N mutant. A second ESC line and a mouse line were generated by correction of the *ΔNlrp3* locus with the D305N *NLRP3*-containing DNA fragment. Mice were housed within a specific pathogen-free animal facility. Control mice were either littermates or mice matched and co-housed at weaning with control animals bred in the same room. Studies were conducted in accordance with the NIH Guide for the Care and Use of Laboratory Animals and the Institutional Animal Care and Use Committee guidelines for the University of North Carolina at Chapel Hill.

Expression Analysis

RNA was isolated using RNA-Bee (Tel-Test), and cDNA was generated with a high-capacity cDNA archive kit (Applied Biosystems). cDNA was amplified with Taqman PCR Universal Master Mix using commercially available probes/primers (Applied Biosystems). Samples were run in duplicate, and relative expression was determined by normalizing samples to 18S RNA (ΔC_T). Data were analyzed using the comparative C_T method as described by Applied Biosystems. In some experiments, samples from mutant animals were normalized to values obtained from co-housed control animals ($\Delta\Delta C_T$).

Activation of Macrophages

Macrophages were cultured in RPMI medium containing 10% fetal bovine serum (FBS), 10 mM 4-(2-hydroxyethyl)-1-piperazineethanesulfonic acid (HEPES), L-glutamine, penicillin/streptomycin (pen/strep), and 2-mercaptoethanol with LPS alone (*E. coli* serotype 055:B5, 1 μg/mL unless otherwise indicated) or LPS plus one of the following agents: silica (250 μg/mL), MSU (100–500 μg/mL), CPPD (100–500 μg/mL), R837 (5 μg/mL), or R848 (5 μg/mL). ATP (5 mM) or nigericin (20 μM) was added to LPS-treated cultures 30 min before harvest. In some experiments, macrophages were collected 72 hr after treatment of mice with 2.5 mL of 4% thioglycollate broth.

LPS-Induced Hypothermia

Mice received the indicated LPS dose i.p. in saline. The core body temperature was measured using a rectal probe (Physitemp Instruments). Peritoneal exudate was collected from the peritoneal cavity after injection of 3 mL of PBS. In some experiments, mice were treated with CRID3/MCC950, catalog no. 210826-40-7, dissolved in saline, i.p. 30 min before LPS exposure.

Quantification of Cytokines and Inflammatory Mediators

ELISA was used to quantify IL-1α, IL-1β, TNF-α, and IL-6 (eBioscience); IL-18 and IL-1ra (R&D Systems); and serum amyloid (Immunology Consultants Laboratory). Homogenates were prepared from hindpaws, including the tarsus, as described previously (Lu et al., 2010) using Fast Prep24 126-48 and Roche protease inhibitor cocktail tablets.

Edema Formation

Evan's blue (0.05% in PBS) was delivered intravenously (i.v.) (0.01mL/g). 30 min later, mice were euthanized, tissue was collected, and extravasated dye was extracted in formamide at 55°C and quantitated by spectrophotometry at 610 nm as described.

Flow Cytometry

Flow cytometry was performed using a Beckman Coulter CyAn ADP analyzer, and data were analyzed using FloJo (TreeStar) software after staining with CD4-FITC, CD8-PE, CD69-APC, or isotype-matched control antibodies (BD Biosciences).

Non-invasive Monitoring of Inflammation and Bone Loss

Animals received 200 mg/kg of chemiluminescent reagent (XenoLight Rediject Probe, PerkinElmer) by i.v. injection. Images were captured 5 min later using an indocyanine green (ICG) filter set for IVIS Lumina. Radiographic images were obtained using a Faxitron X-ray MX-20 specimen radiograph system (10 s at 18 kV) and analyzed with Agfa CR-35X digital X-ray. For microCT imaging and bone analysis, the left hindlimbs of 6-month-old female mice were imaged in 70% ethanol with the knee joint intact using microCT at a resolution of 10 μm (μct80, Scanco Medical). The trabecular bone microarchitecture was

analyzed in the proximal tibia metaphysis in a region beginning just distal to the epiphyseal growth plate and extending 1 mm in length away from the knee joint.

Isolation of Peritoneal Mast Cells

Peritoneal cells were collected by lavage, and mast cells were purified by Percoll density centrifugation as described previously (Hachisuka et al., 1988). The purity of the cell populations was determined to be greater than 99% based on staining of a sample of cells with toluidine.

Western Blot Analysis

Macrophages were stimulated with 1 μg/mL LPS and lysed at the indicated time. 20 μg of total protein was separated by SDS-PAGE (Hybond-P, Amersham, GE Healthcare) under reducing conditions, transferred onto a polyvinylidene difluoride membrane, and incubated with an antibody that can bind both human and mouse NLRP3 (Cryo-2 Adipogen) and anti-mouse-IgG HRP (#7076) from Cell Signaling Technology.

Statistical Analysis

Unless otherwise indicated in the figure legends, groups were compared by two-tailed Student's t test.

SUPPLEMENTAL INFORMATION

Supplemental Information includes Supplemental Experimental Procedures, six figures, and two tables and can be found with this article online at http://dx.doi.org/10.1016/j.celrep.2016.11.052.

AUTHOR CONTRIBUTIONS

Conceptualization, J.N.S., J.P.-Y.T., B.E.B., T.A.B., and B.H.K; Methodology, M.N., J.N.S., and B.K.; Formal Analysis, M.N., P.W.R., M.K., and B.E.B.; Investigation, M.N., J.N.S., P.W.R., M.K., E.W.L., R.D., and B.E.B.; Writing – Original Draft, J.N.S., B.E.B., T.A.B., S.S.M., and B.H.K.; Writing – Review & Editing, J.N.S.; Visualization, M.N., J.N.S., P.W.R., M.K., B.E.B., and B.H.K; Supervision Oversight, B.H.K.; Funding Acquisition, B.H.K.

ACKNOWLEDGMENTS

We thank Anne Latour for assistance with tissue culture and Joseph Snouwaert for artwork. This work was supported by NIH grants AR061491 (to B.H.K.), U54HD079124 (to S.S.M.), and R37-A1029564, CA156330, DK094779, and AI067798 (to J.P.-Y.T.).

Received: November 22, 2015
Revised: August 29, 2016
Accepted: November 16, 2016
Published: December 13, 2016

REFERENCES

Agostini, L., Martinon, F., Burns, K., McDermott, M.F., Hawkins, P.N., and Tschopp, J. (2004). NALP3 forms an IL-1beta-processing inflammasome with increased activity in Muckle-Wells autoinflammatory disorder. Immunity *20*, 319–325.

Aksentijevich, I., Nowak, M., Mallah, M., Chae, J.J., Watford, W.T., Hofmann, S.R., Stein, L., Russo, R., Goldsmith, D., Dent, P., et al. (2002). De novo CIAS1 mutations, cytokine activation, and evidence for genetic heterogeneity in patients with neonatal-onset multisystem inflammatory disease (NOMID): a new member of the expanding family of pyrin-associated autoinflammatory diseases. Arthritis Rheum. *46*, 3340–3348.

Aksentijevich, I., D Putnam, C., Remmers, E.F., Mueller, J.L., Le, J., Kolodner, R.D., Moak, Z., Chuang, M., Austin, F., Goldbach-Mansky, R., Hoffman, H.M., and Kastner, D.L. (2007). The clinical continuum of cryopyrinopathies: novel CIAS1 mutations in North American patients and a new cryopyrin model. Arthritis Rheum. *56*, 1273–1285.

Aksentijevich, I., Masters, S.L., Ferguson, P.J., Dancey, P., Frenkel, J., van Royen-Kerkhoff, A., Laxer, R., Tedgård, U., Cowen, E.W., Pham, T.H., et al. (2009). An autoinflammatory disease with deficiency of the interleukin-1-receptor antagonist. N. Engl. J. Med. *360*, 2426–2437.

Anderson, J.P., Mueller, J.L., Rosengren, S., Boyle, D.L., Schaner, P., Cannon, S.B., Goodyear, C.S., and Hoffman, H.M. (2004). Structural, expression, and evolutionary analysis of mouse CIAS1. Gene *338*, 25–34.

Anderson, J.P., Mueller, J.L., Misaghi, A., Anderson, S., Sivagnanam, M., Kolodner, R.D., and Hoffman, H.M. (2008). Initial description of the human NLRP3 promoter. Genes Immun. *9*, 721–726.

Atianand, M.K., Duffy, E.B., Shah, A., Kar, S., Malik, M., and Harton, J.A. (2011). Francisella tularensis reveals a disparity between human and mouse NLRP3 inflammasome activation. J. Biol. Chem. *286*, 39033–39042.

Baresić, A., Hopcroft, L.E., Rogers, H.H., Hurst, J.M., and Martin, A.C. (2010). Compensated pathogenic deviations: analysis of structural effects. J. Mol. Biol. *396*, 19–30.

Bonar, S.L., Brydges, S.D., Mueller, J.L., McGeough, M.D., Pena, C., Chen, D., Grimston, S.K., Hickman-Brecks, C.L., Ravindran, S., McAlinden, A., et al. (2012). Constitutively activated NLRP3 inflammasome causes inflammation and abnormal skeletal development in mice. PLoS ONE *7*, e35979.

Brydges, S.D., Mueller, J.L., McGeough, M.D., Pena, C.A., Misaghi, A., Gandhi, C., Putnam, C.D., Boyle, D.L., Firestein, G.S., Horner, A.A., et al. (2009). Inflammasome-mediated disease animal models reveal roles for innate but not adaptive immunity. Immunity *30*, 875–887.

Camps, M., Herman, A., Loh, E., and Loeb, L.A. (2007). Genetic constraints on protein evolution. Crit. Rev. Biochem. Mol. Biol. *42*, 313–326.

Cassel, S.L., Eisenbarth, S.C., Iyer, S.S., Sadler, J.J., Colegio, O.R., Tephly, L.A., Carter, A.B., Rothman, P.B., Flavell, R.A., and Sutterwala, F.S. (2008). The Nalp3 inflammasome is essential for the development of silicosis. Proc. Natl. Acad. Sci. USA *105*, 9035–9040.

Church, L.D., Savic, S., and McDermott, M.F. (2008). Long term management of patients with cryopyrin-associated periodic syndromes (CAPS): focus on rilonacept (IL-1 Trap). Biologics *2*, 733–742.

Dinarello, C.A. (2009). Immunological and inflammatory functions of the interleukin-1 family. Annu. Rev. Immunol. *27*, 519–550.

Elliott, E.I., and Sutterwala, F.S. (2015). Initiation and perpetuation of NLRP3 inflammasome activation and assembly. Immunol. Rev. *265*, 35–52.

Feldmann, J., Prieur, A.M., Quartier, P., Berquin, P., Certain, S., Cortis, E., Teillac-Hamel, D., Fischer, A., and de Saint Basile, G. (2002). Chronic infantile neurological cutaneous and articular syndrome is caused by mutations in CIAS1, a gene highly expressed in polymorphonuclear cells and chondrocytes. Am. J. Hum. Genet. *71*, 198–203.

Hachisuka, H., Kusuhara, M., Higuchi, M., Okubo, K., and Sasai, Y. (1988). Purification of rat cutaneous mast cells with Percoll density centrifugation. Arch. Dermatol. Res. *280*, 358–362.

Horai, R., Saijo, S., Tanioka, H., Nakae, S., Sudo, K., Okahara, A., Ikuse, T., Asano, M., and Iwakura, Y. (2000). Development of chronic inflammatory arthropathy resembling rheumatoid arthritis in interleukin 1 receptor antagonist-deficient mice. J. Exp. Med. *191*, 313–320.

Kanneganti, T.D., Ozören, N., Body-Malapel, M., Amer, A., Park, J.H., Franchi, L., Whitfield, J., Barchet, W., Colonna, M., Vandenabeele, P., et al. (2006). Bacterial RNA and small antiviral compounds activate caspase-1 through cryopyrin/Nalp3. Nature *440*, 233–236.

Kastner, D.L., Aksentijevich, I., and Goldbach-Mansky, R. (2010). Autoinflammatory disease reloaded: a clinical perspective. Cell *140*, 784–790.

Kondrashov, A.S., Sunyaev, S., and Kondrashov, F.A. (2002). Dobzhansky-Muller incompatibilities in protein evolution. Proc. Natl. Acad. Sci. USA *99*, 14878–14883.

Kovarova, M., Hesker, P.R., Jania, L., Nguyen, M., Snouwaert, J.N., Xiang, Z., Lommatzsch, S.E., Huang, M.T., Ting, J.P., and Koller, B.H. (2012). NLRP1-dependent pyroptosis leads to acute lung injury and morbidity in mice. J. Immunol. *189*, 2006–2016.

Leemans, J.C., Cassel, S.L., and Sutterwala, F.S. (2011). Sensing damage by the NLRP3 inflammasome. Immunol. Rev. *243*, 152–162.

Lehner, B. (2011). Molecular mechanisms of epistasis within and between genes. Trends Genet. *27*, 323–331.

Lu, L.D., Stump, K.L., and Seavey, M.M. (2010). Novel method of monitoring trace cytokines and activated STAT molecules in the paws of arthritic mice using multiplex bead technology. BMC Immunol. *11*, 55.

Manji, G.A., Wang, L., Geddes, B.J., Brown, M., Merriam, S., Al-Garawi, A., Mak, S., Lora, J.M., Briskin, M., Jurman, M., et al. (2002). PYPAF1, a PYRIN-containing Apaf1-like protein that assembles with ASC and regulates activation of NF-kappa B. J. Biol. Chem. *277*, 11570–11575.

Martinon, F., Burns, K., and Tschopp, J. (2002). The inflammasome: a molecular platform triggering activation of inflammatory caspases and processing of proIL-beta. Mol. Cell *10*, 417–426.

Martinon, F., Pétrilli, V., Mayor, A., Tardivel, A., and Tschopp, J. (2006). Gout-associated uric acid crystals activate the NALP3 inflammasome. Nature *440*, 237–241.

Meng, G., Zhang, F., Fuss, I., Kitani, A., and Strober, W. (2009). A mutation in the Nlrp3 gene causing inflammasome hyperactivation potentiates Th17 cell-dominant immune responses. Immunity *30*, 860–874.

Nicklin, M.J., Hughes, D.E., Barton, J.L., Ure, J.M., and Duff, G.W. (2000). Arterial inflammation in mice lacking the interleukin 1 receptor antagonist gene. J. Exp. Med. *191*, 303–312.

Ostedgaard, L.S., Rogers, C.S., Dong, Q., Randak, C.O., Vermeer, D.W., Rokhlina, T., Karp, P.H., and Welsh, M.J. (2007). Processing and function of CFTR-DeltaF508 are species-dependent. Proc. Natl. Acad. Sci. USA *104*, 15370–15375.

Pasparakis, M., Haase, I., and Nestle, F.O. (2014). Mechanisms regulating skin immunity and inflammation. Nat. Rev. Immunol. *14*, 289–301.

Reddy, S., Jia, S., Geoffrey, R., Lorier, R., Suchi, M., Broeckel, U., Hessner, M.J., and Verbsky, J. (2009). An autoinflammatory disease due to homozygous deletion of the IL1RN locus. N. Engl. J. Med. *360*, 2438–2444.

Redlich, K., and Smolen, J.S. (2012). Inflammatory bone loss: pathogenesis and therapeutic intervention. Nat. Rev. Drug Discov. *11*, 234–250.

Solle, M., Labasi, J., Perregaux, D.G., Stam, E., Petrushova, N., Koller, B.H., Griffiths, R.J., and Gabel, C.A. (2001). Altered cytokine production in mice lacking P2X(7) receptors. J. Biol. Chem. *276*, 125–132.

Stojanov, S., and Kastner, D.L. (2005). Familial autoinflammatory diseases: genetics, pathogenesis and treatment. Curr. Opin. Rheumatol. *17*, 586–599.

Ting, J.P., Lovering, R.C., Alnemri, E.S., Bertin, J., Boss, J.M., Davis, B.K., Flavell, R.A., Girardin, S.E., Godzik, A., Harton, J.A., et al. (2008). The NLR gene family: a standard nomenclature. Immunity *28*, 285–287.